JOURNAL OF CATALYSIS 137, 267–277 (1992)

Two Promoting Effects of Gadolinium on Ni/SiO_2 Catalysis for CO Hydrogenation

TAKAFUMI SHIDO[1] AND YASUHIRO IWASAWA[2]

Department of Chemistry, Faculty of Science, the University of Tokyo, Hongo, Bunkyo-ku, Tokyo 113, Japan

Received February 10, 1992; revised April 29, 1992

Promoting effects of Gd and CO–H interaction in CO hydrogenation on $Ni/Gd/SiO_2$ catalysts have been investigated by means of kinetics, TPR, and FT–IR. The reaction rate of CO hydrogenation on $Ni/Gd/SiO_2$ was about five times faster than that on Ni/SiO_2 above 500 K. The IR band of side-on CO (Ni–C=O–Gd) on $Ni/Gd/SiO_2$ was observed at 1600 cm^{-1} in addition to the bands of on-top (ca. 2040 cm^{-1}) and bridge CO (ca. 1950 cm^{-1}). All side-on CO easily dissociates, whereas most on-top Gd exists as partially reduced GdO_x and the GdO_x acts as a reservoir of hydrogen. A new peak due to Gd–H was observed at 1610 cm^{-1} under reaction conditions. The adsorbed hydrogen increased the amount of CO adsorbed on $Ni/Gd/SiO_2$. Consequently, the easy dissociation of CO and the storage of hydrogen on the $Ni/Gd/SiO_2$ catalyst promoted the hydrogenation of CO to hydrocarbons (mainly methane). © 1992 Academic Press, Inc.

INTRODUCTION

In important catalytic reactions, such as CO hydrogenation (*1–3*), oxidative coupling of methane (*4*), and NO–CO reaction (*5*), the addition of rare earth metals increases the catalytic activities. Vannice and co-workers (*1, 2*) found that the activity of methanation over Pd supported on rare earth oxides (REO) is 10 times larger than that over Pd/SiO_2. Rieck and Bell (*3*) investigated the adsorbed states of H_2 and CO by TPD and TPR on REO's doped Pd/SiO_2 (*3*). They suggested that partially reduced REO is decorated on Pd particles and that REO promotes CO dissociation by forming side-on CO (Pd–C=O–M). IR spectra of adsorbed CO on several REO-doped transition metal catalysts have been measured (*6–10*). On Ce-doped Rh/SiO_2, Kienneman *et al.* (*6*) observed a band at 1725 cm^{-1} in addition to the bands of on-top, bridge, and twin CO and assigned the low-frequency band to be side-on CO. The low-frequency CO has been believed to be a precursor to the dissociation of CO.

Nickel is known as a good methanation catalyst, and this reaction is thought to proceed through CO dissociation and the subsequent hydrogenation of carbide (*11, 12*). Chung *et al.* investigated CO chemisorption on Ni(111) surfaces which are modified by partially reduced MnO_x (*13*) and AlO_x (*14*) by means of HREELS, and they found that low-frequency bands at ca. 1620 cm^{-1} for both modified the Ni(111) systems. Yates and co-workers (*15, 16*) studied CO chemisorption on Ni/Al(111) by HREELS and they found a low-frequency band at 1370–1430 cm^{-1} which they attributed to Ni_x–C–O–Al_y. Thus, by the addition of REOs to Ni systems, it is expected that the dissociation of CO is promoted similarly to the cases of Pd/REO and that the activity for methanation is enhanced.

We investigated the activities of Ni catalysts supported on several REOs, such as La_2O_3, CeO_2, Gd_2O_3, and Er_2O_3 oxide for

[1] Present address: Catalysis Research Center, Hokkaido University, Sapporo 060, Japan.

[2] To whom correspondence should be addressed.

0021-9517/92 $5.00
Copyright © 1992 by Academic Press, Inc.
All rights of reproduction in any form reserved.

CO hydrogenation, and found that Ni/Gd_2O_3 shows the highest activity. It is difficult to characterize Ni/Gd_2O_3 catalysts by IR and EXAFS because of the strong absorption of IR and X ray by Gd_2O_3. Hence, in this paper we used Ni–Gd coimpregnate catalysts for less spectroscopic interference.

We have demonstrated the promotion of catalytic and surface reactions induced by coadsorbates (*17–20*). The present study reports the promoter effect of Gd additive on Ni catalysis for CO hydrogenation in relation to the behavior and interaction of adsorbates.

EXPERIMENTAL

Ni and Gd were coimpregnated on SiO_2 (Aerosil 200) using aqueous solution of $Ni(NO_3)_2 \cdot 6H_2O$ (99%, Soekawa Co., Ltd.) and $Gd_2(NO_3)_2$ (99%, Soekawa), where the content of Ni in the catalysts was fixed at 1.5 wt%, while the amount of Gd was varied. Then the samples were dried, ground into fine powders, and calcined at 650 K. Before use as catalysts, the samples were oxidized in 13 kPa of oxygen at 673 K for 1 h and reduced in 13 kPa of hydrogen at 773 K for 1.5 h. While Ni/SiO_2 represents Ni catalysts supported on SiO_2, Ni/Gd(X)/SiO_2 represents Ni–Gd—coimpregnated catalysts on SiO_2 with Ni 1.5 wt% and Gd(X) wt%. Gd_2O_3 was obtained by calcination of $Gd(OH)_3$ (99%, Soekawa) at 673 K for 3 h in air. Gd/SiO_2 (5 wt%) was obtained by impregnation of $Gd(NO_3)_2$ on Aerosil 200 and treated in a way similar to that for Ni/Gd/SiO_2.

Commercially obtained H_2 (99.9999%), CO (99.99%), and ^{13}CO (isotope purity of 99%) were used after purification through a liquid N_2 trap.

The amounts of adsorbed CO and hydrogen were volumetrically measured at room temperature. Samples were exposed to 13 kPa of CO or hydrogen and the adsorbed amounts were measured (M_1 μmol g_{cat}^{-1}). Then the samples were evacuated for 30 min and the second adsorption was measured again (M_2 μmol g_{cat}^{-1}). The amount of irreversible adsorption was obtained by the difference ($M_1 - M_2$).

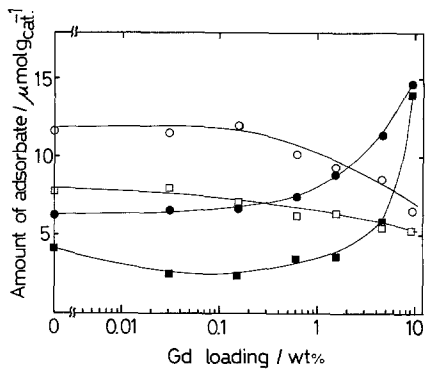

FIG. 1. Adsorbed amounts of hydrogen and CO as a function of Gd loading. (○) Irreversibly adsorbed CO; (●) reversibly adsorbed CO; (□) irreversibly adsorbed H_2; (■) reversibly adsorbed H_2.

Reaction products and desorbed species were analyzed by mass spectrometry (Ulvac MSQ-150A) and/or gas chromatography (Simazu GC-8A). The columns of the Porapak R and the 5 A molecular sieve were used at 353 K for the detection of CO_2, C_2H_6, C_3H_8, and H_2O and for H_2, CO, and CH_4, respectively.

IR measurements were conducted in a way similar to that previously described (*17, 21*). Ni/Gd/SiO_2 catalysts (ca. 30 mg) were pressed into self-supported discs (ϕ = 20 mm). Then a disc was set in a quartz IR cell with two NaCl windows and pretreated in the same way as that for kinetic studies. IR spectra were measured at room temperature or reaction temperatures with a resolution of 2 or 4 cm^{-1}.

RESULTS

1. Adsorbed Amounts of CO and Hydrogen

Figure 1 shows adsorbed amounts of CO and hydrogen as a function of Gd loading. The amount of CO and hydrogen irreversibly adsorbed decreased as Gd loading increased. The amount of CO irreversibly adsorbed on Ni/SiO_2 was 11.6 μmol g_{cat}^{-1}. It

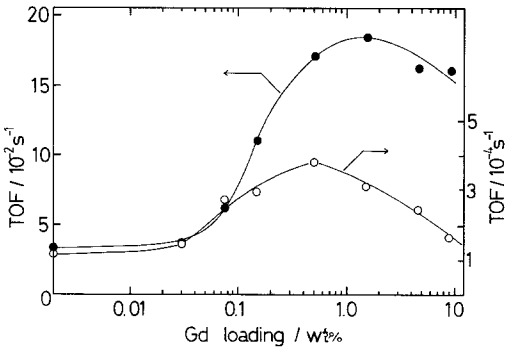

FIG. 2. Rates of methane formation at 433 K (○) and 538 K (●) as a function of Gd loading; $p(CO)$ = 4.0 kPa, $p(H_2)$ = 21.3 kPa.

began to decrease at 0.1 wt% of Gd loading and reached 7.0 μmol g_{cat}^{-1} at 9 wt% Gd. Reversibly adsorbed CO increased with an increase of Gd loading and became 15 μmol g_{cat}^{-1} at 9 wt% Gd, which is about twice as large as that for Ni/SiO_2.

2. *TEM and EXAFS*

Averaged particle sizes of Ni particles in Ni/SiO_2 and $Ni/Gd(1.5)/SiO_2$ were determined to be 7.0 and 6.6 nm, respectively, by TEM measurements. Gd L_{III} edge EXAFS showed only Gd–O bond at 0.20 nm, and neither Gd–Gd nor Gd–Ni bonds were observed. As the Ni K edge (8.26 keV) is close to the Gd L_1 edge (8.39 keV), we cannot reasonably obtain EXAFS spectra of the Ni K edge.

3. *Kinetic Study*

Figure 2 shows turnover frequencies (TOF) for methane formation from CO/H_2 syngas as a function of Gd loading. The TOFs in this study are based on the irreversible adsorption of H_2. The maximum activity at 433 K was obtained with $Ni/Gd(0.5)/SiO_2$. The activity of $Ni/Gd/SiO_2$ at maximum was 2.5 times larger than that of Ni/SiO_2. At 538 K, the TOF had a maximum at 1.5 wt% of Gd. The maximum value was six times larger than that of Ni/SiO_2. The difference of maximum TOF of $Ni/Gd/SiO_2$ and the TOF of Ni/SiO_2 was larger at 538 K than that at 433 K. At higher Gd loadings beyond the optimum loadings at 433 and 538 K, the TOFs decreased. The extent of the decrease of rate with an increase of Gd loading at 433 K was larger than that at 538 K.

Figure 3 shows Arrhenius plots of CO hydrogenation on Ni/SiO_2 and $Ni/Gd(1.5)/SiO_2$ catalysts. For Ni/SiO_2, the rate of C_2H_6 and C_3H_8 formation decreased as the temperature increased to above 500 K, and the activation energy for CH_4 formation changed from 121 kJ mol^{-1} below 500 K to 79 kJ mol^{-1} above 500 K. For $Ni/Gd(1.5)/SiO_2$, the activation energy for CH_4 formation did not change in this temperature range, and the decrease in the rates of C_2H_6 and C_3H_8 formations at high temperatures was not as large as that for Ni/SiO_2, as shown in Fig. 3.

Figure 4 shows the rate of methane formation as a function of the partial pressure of CO ($p(CO)$). On Ni/SiO_2, the maximum rate was observed at $p(CO)$ = 0.13 kPa and the rate was proportional to $p(CO)^{-0.90}$ above 0.13 kPa. On the other hand, the rate

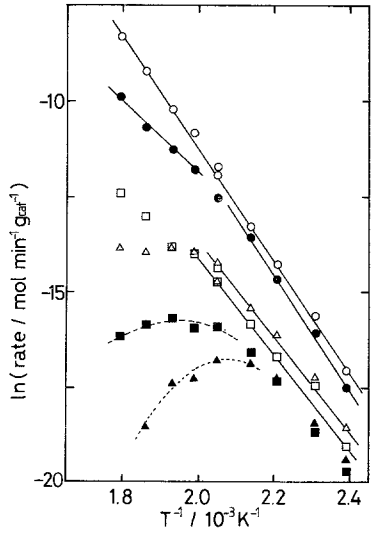

FIG. 3. Arrhenius plots for the formations of methane, ethane, and propane on $Ni/Gd/SiO_2$ (○,□,△) and Ni/SiO_2 (●,■,▲); (○,●) methane; (□,■) ethane; (△,▲) propane.

of methane formation on Ni/Gd(1.5)/SiO_2 was proportional to $p(CO)^{-0.67}$ in the whole range of $p(CO)$ in Fig. 4.

4. TPR Study

Figure 5 shows TPR spectra of adsorbed CO on (A) Ni/Gd(1.5)/SiO_2 and (B) Ni/SiO_2. The sample was exposed to CO (4.0 kPa) at 300 K, followed by evacuation. Then the samples were exposed to 3.3 kPa of H_2, followed by heating at a heating rate of 4 K min^{-1}. For Ni/SiO_2, the desorption peak of methane at 465 K was observed and that of CO was observed at 430 K. No CO_2 was observed. On the other hand, for Ni/Gd(1.5)/SiO_2, the desorption peak of methane at 445 K was observed and that of CO_2 instead of CO was observed at 410 K. The amount of water desorbed was not quantitatively measured because of the experimental restriction.

Figures 6A and 6B show TPR spectra of surface carbides on Ni/Gd(1.5)/SiO_2 and Ni/SiO_2, respectively. The samples were exposed to CO (4.0 kPa) at 523 K, followed by evacuation, to form surface carbides by the Boudward reaction. The samples were exposed to 3.3 kPa of H_2, followed by heating at a rate of 4 K min^{-1}. For Ni/SiO_2, CH_4 was desorbed at 405 and 465 K. The desorption peak of 465 K corresponds to the CH_4 peak in Fig. 5B, because a certain amount of CO remained on Ni/SiO_2 after evacuation at 523 K as proved by IR. As for Ni/Gd(1.5)/SiO_2 a desorption peak of CH_4 at 445 K was observed. Small amounts of C_2H_6 and C_3H_8 were desorbed at the same temperature.

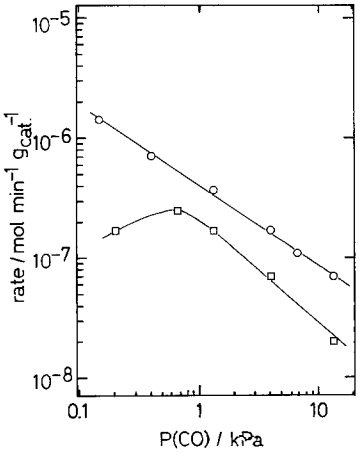

FIG. 4. Rates of methane formation at 433 K as a function of $p(CO)$ on Ni/Gd(1.5)/SiO_2 (○) and Ni/SiO_2 (□); $p(H_2)$ = 21.3 kPa.

Figure 7 shows TPR spectra from Ni/Gd(1.5)/SiO_2 having ^{12}C-labeled carbide and ^{13}CO. The sample was exposed to 4.0 kPa of ^{12}CO at 300 K, followed by evacuation at 500 K for 30 min, and then cooled to 300 K. The sample was further exposed to 4.0 kPa of ^{13}CO, followed by evacuation. The TPR spectra were measured in the presence of 0.6 kPa of hydrogen at a heating rate of 4.0 K min^{-1}. $^{13}CH_4$ and $^{12}CH_4$ were evolved at 480 and 465 K, respectively. The amounts of $^{13}CH_4$ and $^{12}CH_4$ produced are 7.1 and 1.9 $\mu mol\ g_{cat}^{-1}$, respectively.

5. IR Study

Ni/SiO_2 and Ni/Gd(1.5)/SiO_2 were exposed to CO (4.0 kPa) at 303 K, followed by evacuation at given temperatures for 30 min. The IR spectra in Figs. 8A and 8B were recorded at room temperature. Ni/SiO_2 exhibited the bands at 2040–2030 and 1950–1800 cm^{-1}. The peak at 2030 cm^{-1} began to decrease at 500 K, while the peak at 1950 cm^{-1} already decreased at 343 K. The peaks due to adsorbed CO almost vanished at 543 K. When the sample was exposed to CO at 303 K again, IR bands appeared at 2040 (with a shoulder at 2062 cm^{-1}) and 1950 cm^{-1}. The total band intensity was almost the same as that of the fresh Ni/SiO_2 catalyst. On the other hand, three strong bands at 2070, 2030, and 1950 cm^{-1} and a weak band at 1600 cm^{-1} were observed with Ni/Gd(1.5)/SiO_2. The new peak of 1600 cm^{-1} began to decrease at 353 K. The bands at 2070, 2030, and 1950 cm^{-1} decreased at 423 K and vanished at 503 K. When Ni/Gd(1.5)/SiO_2 was exposed to CO at 303 K again, the bands at 2070, 2030, and 1950 cm^{-1} appeared again; in

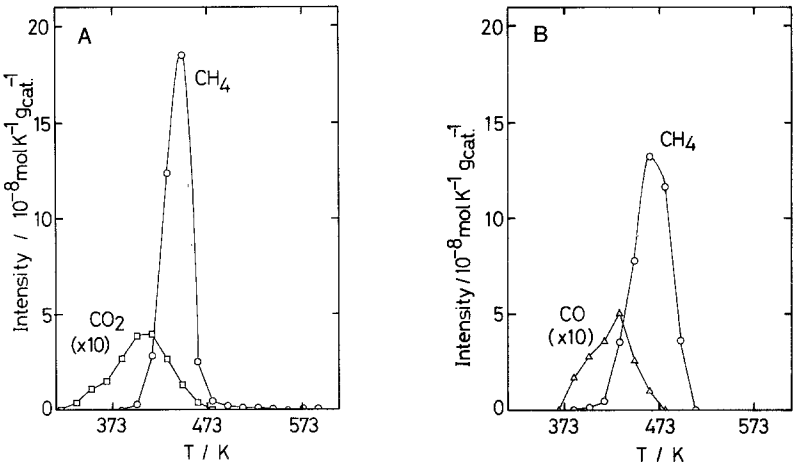

FIG. 5. (A) TPR spectra of adsorbed CO on Ni/Gd(1.5)/SiO$_2$ in the presence of $p(H_2)$ = 3.3 kPa; heating rate = 4 K min^{-1}. (B) TPR spectra of adsorbed CO on Ni/SiO$_2$ in the presence of $p(H_2)$ = 3.3 kPa; heating rate = 4 K min^{-1}.

contrast, the peak of 1600 cm^{-1} no longer appeared.

When Ni/Gd(1.5)/SiO$_2$ was exposed to 4.0 kPa of hydrogen at 403 K, an IR peak at 1610 cm^{-1} was observed, as shown in Fig. 9. The intensity gradually increased with the exposure time and reached an equilibrium at 30 min. When 0.40 kPa of CO was introduced to the system without evacuating H_2 at 403 K, the peak intensity at 1610 cm^{-1} immediately increased and became twice as large as that before CO exposure. The peak position did not shift by replacing ^{12}CO by ^{13}CO. This band disappeared by exposure to D_2. The amount of hydrogen adsorbed on the catalyst corresponding to the spectrum (d) or the spectrum (h) in Fig. 9 was determined by the temperature-programmed desorption measurements by mass spectrometry: 0.08 μmol g_{cat}^{-1} of hydrogen for the sample after exposure to 4.0 kPa of hydrogen for 30 min and 0.14 μmol g_{cat}^{-1} for the

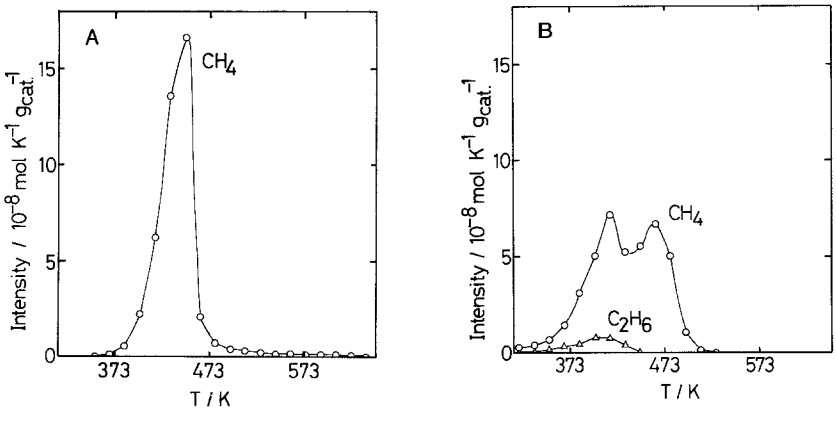

FIG. 6. (A) TPR spectra of surface carbide on Ni/Gd(1.5)/SiO$_2$ in the presence of $p(H_2)$ = 3.3 kPa; heating rate = 4 K min^{-1}. (B) TPR spectra of surface carbide on Ni/SiO$_2$ in the presence of $p(H_2)$ = 3.3 kPa; heating rate = 4 K min^{-1}.

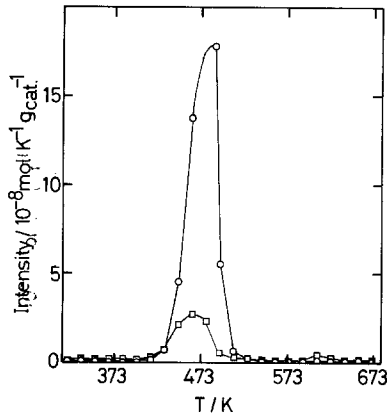

FIG. 7. TPR spectra of ^{12}C-labeled carbide and ^{13}CO on $Ni/Gd(1.5)/SiO_2$. The sample was exposed to ^{12}CO at 300 K followed by evacuation at 500 K to form carbides. The sample was then exposed to ^{13}CO at 300 K, followed by evacuation at the same temperature. The TPR spectrum was measured in the presence of 0.6 kPa of hydrogen; heating rate = 4 K min^{-1}. (○) $^{13}CH_4$; (□) $^{12}CH_4$.

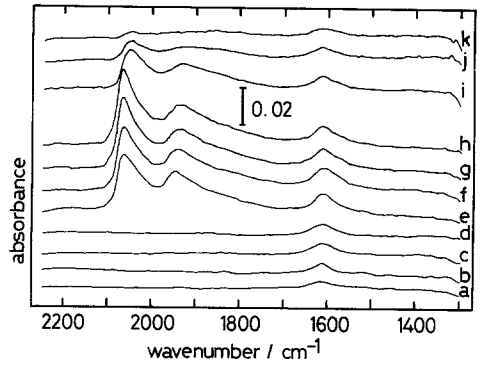

FIG. 9. IR spectra of adsorbed hydrogen without and with coadsorbed CO on $Ni/Gd(1.5)/SiO_2$. IR spectra were measured at 403 K. The sample was exposed to 4.0 kPa of H_2 at 403 K for (a) 2.5 min, (b) 10 min, (c) 20 min, and (d) 30 min. After (d), without evacuation, the sample was further exposed to 0.23 kPa of CO at 403 K for (e) 2.5 min, (f) 10 min, (g) 20 min, and (h) 30 min. After (h), the sample was evacuated for (i) 10 min, (j) 30 min, and (k) 60 min.

sample after exposure to 0.40 kPa of CO for 30 min following the H_2 exposure.

Figure 10 shows IR spectra of CO adsorbed on Gd/SiO_2. When the sample reduced at 773 K for 1 h was exposed to CO at 303 K, IR bands at 2191, 2138, 2085, 2017, 1950, and 1857 cm^{-1} appeared, as shown in Fig. 10. By evacuation at 303 K, the bands at 2191, 2138, 2017, and 1950 cm^{-1} disappeared, showing the remaining two peaks at 2077 and 1857 cm^{-1}. For the sample reduced for 2.5 h, the spectrum was more intense, but the feature was similar to that for the 1-h-reduced sample. The amount of CO re-

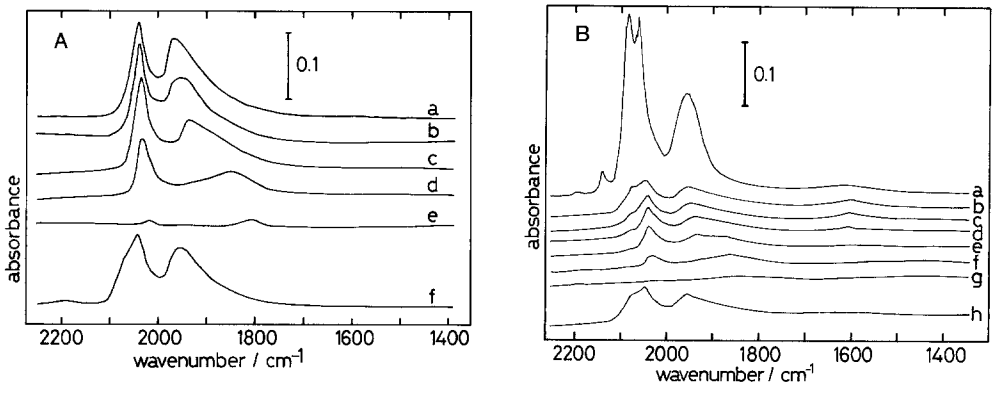

FIG. 8. (A) IR spectra of adsorbed CO on Ni/SiO_2. The sample was exposed to 4.0 kPa of CO at 303 K, followed by evacuation at (a) 303 K, (b) 343 K, (c) 423 K, (d) 503 K, and (e) 543 K. After (e), the sample was exposed to 4.0 kPa of CO at 303 K again, followed by evacuation at 303 K (f). (B) IR spectra of adsorbed CO on $Ni/Gd(1.5)/SiO_2$. The sample was exposed to 4.0 kPa of CO at 303 K (a) followed by evacuation at (b) 303 K, (c) 343 K, (d) 383 K, (e) 423 K, (f) 463 K, and (g) 503 K. After (g), the sample was exposed to 4.0 kPa of CO at 303 K again, followed by evacuation at 303 K(h).

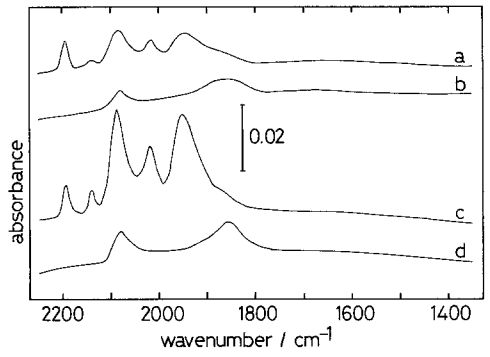

FIG. 10. IR spectra of adsorbed CO on Gd/SiO_2. The sample reduced at 773 K for 1 h was exposed to 4.0 kPa of CO at 303 K (a), followed by evacuation at 303 K (b). The sample reduced at 773 K for 4 h was exposed to 4.0 kPa of CO at 303 K (c), followed by evacuation at 303 K (d).

versibly adsorbed CO on the 2.5-h-reduced sample is about four times larger than that for the 1-h-reduced sample, and the amount of CO irreversibly adsorbed for the 2.5-h-reduced sample is about twice as large as that for the 1-h-reduced sample. The band frequencies of carbonate, carboxylate, and formate adsorbed on Gd_2O_3 are listed in Table 1.

DISCUSSION

1. *Characterization of the Ni/Gd/SiO_2 Catalyst*

The Gd L_{III} edge EXAFS analysis revealed only the presence of the Gd–O bond at 0.20 nm. Neither the Ni–Gd bond nor the Gd–Gd bond was observed. Hence, most Gd atoms may be dispersed as GdO_x particles in an amorphous form. Hydrogen atoms formed on Ni particles in Ni/Gd/SiO_2 reduced with H_2 at 773 K should partially reduce the GdO_x species ($x < 1.5$). This is suggested by the fact that adsorbed CO on GdO_x increases with increasing reduction period, as shown in Fig. 10.

As shown in Fig. 1, the amounts of hydrogen and CO irreversibly adsorbed decreased with an increase of Gd loading, while reversibly adsorbed amounts of them increased. The peak frequencies of reversibly adsorbed CO on Ni/Gd/SiO_2 are almost the same as those of reversibly adsorbed CO on GdO_x/SiO_2, as shown in Figs. 8B and 10. On the other hand, irreversibly adsorbed CO on Ni/Gd/SiO_2 showed similar frequencies to those of CO irreversibly adsorbed on Ni/SiO_2. These facts suggest that CO and hydrogen strongly adsorbed on Ni particles, but weakly adsorb on partially reduced GdO_x.

According to TEM measurements, Ni particle size in Ni/Gd/SiO_2 was independent of Gd loading. Thus the decrease of irreversible CO quantity in Fig. 1 is suggested to be due not to the decrease of the dispersion of Ni particle but to the deposition of GdO_x on Ni particles. The amount of Ni–C=O–Gd (1.9 μmol g_{cat}^{-1} for Ni/Gd(1.5)/SiO_2 as discussed hereinafter) was almost the same as the decrease of Ni surface area (2.1 μmol g_{cat}^{-1} for Ni/Gd(1.5)/SiO_2), which demonstrates that a part of the GdO_x species migrated on Ni particles to be dispersed in atomic/small cluster forms.

2. *CO and Carbide Adsorbed on Ni/Gd/SiO_2 and Ni/SiO_2*

When Ni/Gd/SiO_2 was exposed to CO, three absorption bands were observed at 2070–2030, 1980–1900, and 1600 cm^{-1}, as shown in Fig. 8B. The peaks of 2040 and 1950 cm^{-1} are attributed to CO on Nickel metal (*22–24*). On the other hand, as for the low-frequency band at 1600 cm^{-1}, there are two possibilities. One is that the band of surface carbonates or carboxylates on GdO_x particles is ν_{as} (OCO) and the other is that the band is a large red shift of ν(CO) mode

TABLE 1

Frequencies (cm^{-1}) of IR Bands of Adsorbed Species on Gd_2O_3

Species	ν(CD)	ν(C=O)	ν_{as}(OCO)	ν_s(OCO)
Bidentate carbonate		1580	1320	1000
Unidentate carbonate			1477	1389
Carboxylate			1527	1346
Formate	2148		1590	1377

of adsorbed CO. The former possibility is excluded by the fact that ν_{as}(OCO) of carbonates, carboxylates, and formates on Gd_2O_3 appear below 1600 cm^{-1} and that ν_s(OCO) of them which should be in 1400–1000 cm^{-1} was not observed. Similar low-frequency CO has been observed on REO-doped metal catalysts (*6–10*) and Ni surfaces modified by partially reduced oxides (*13–15*). Hence, the peak at 1600 cm^{-1} can be attributed to side-on CO (Ni–C=O–Gd). This peak shifted to 1570 cm^{-1} by ^{13}CO.

As shown in Fig. 8A (f), IR bands at 2040 (with a shoulder at 2062 cm^{-1}) and 1950 cm^{-1} appeared when Ni/SiO_2 was exposed to CO at room temperature after IR bands of adsorbed CO was vanished [Fig. 8A (e)]. The total intensity of the peaks for the second CO adsorption on Ni/SiO_2 is almost the same as that for the first CO adsorption on Ni/SiO_2, which suggests that most of the adsorbed CO on Ni/SiO_2 desorbed when the sample was evacuated up to 543 K. The appearance of a high-frequency band at 2062 cm^{-1} may be attributed to CO adsorbed at morphologically different Ni sites, despite the possibility of adsorbed CO on partially oxidized Ni. IR bands of terminal CO adsorbed on Ni(100) (*25*), Ni(111) (*26*), and Ni[5(111) × (110)] (*27*) appear at 2065, 2045, and 2020–2060 cm^{-1}, respectively. Similarly, on-top and bridge CO molecules on $Ni/Gd(1.5)/SiO_2$ desorb and appear again by CO adsorption [Fig. 8B (h)]. On the contrary, side-on CO on $Ni/Gd(1.5)/SiO_2$ was not reproduced by readsorption of CO at room temperature after evacuation at 503 K. These results show that adsorbed CO on Ni/SiO_2 and on-top and bridge CO on $Ni/Gd(1.5)/SiO_2$ scarcely dissociate by heating to 503–543 K, whereas all of side-on CO on $Ni/Gd/SiO_2$ dissociates. Figure 7 demonstrates the formation of 1.9 μmol g_{cat}^{-1} of $^{12}CH_4$ by the hydrogenation of ^{12}C-labeled carbides originated from the dissociation of side-on CO. The amount of $^{12}CH_4$ was one-fifth as large as that of $^{13}CH_4$ (Fig. 7), which shows that the amount of side-on CO is one-fifth as large as those of on-top and bridge CO.

Without any direct evidence, the side-on CO has been thought to be a precursor for CO dissociation. However, Figs. 7 and 8B provide evidence that side-on CO preferentially dissociates around 400 K to form active carbides for hydrogenation.

By addition of gadolinium, the adsorption of on-top and bridge CO was weakened, as shown in Fig. 8, where on-top and bridge CO on $Ni/Gd/SiO_2$ desorbed at ca. 450 K, but on Ni/SiO_2 CO desorbed at ca. 540 K. This may be caused by the electronic effect of GdO_x because the ν(CO) stretching band of on-top CO blue-shifted by 5–10 cm^{-1}, often leading to a weakening of the Ni–CO bond by a decrease of back donation from Ni to CO due to the electron-withdrawing character of GdO_x on Ni particles. As shown in Fig. 2, the Gd loading in $Ni/Gd/SiO_2$ had an optimum value for promotion of CO hydrogenation, with decreasing TOF at the larger Gd loadings. This decrease of activity may be ascribed to the decrease of side-on sites by aggregation of small GdO_x clusters on Ni particles. In fact, the intensity of the side-on CO peak for the 9 wt% Gd-loaded catalyst was much less than that for the 1.5 wt% loaded catalyst.

3. Interaction of Adsorbed CO and Hydrogen

As shown in Fig. 4, the methanation rate over Ni/SiO_2 depended on $p(CO)^{-0.90}$ in the pressure range $p(CO) > 1.3$ kPa, while that for $Ni/Gd/SiO_2$ depended on $p(CO)^{-0.67}$. This suggests that the suppression/blocking effect of CO is weaker on $Ni/Gd/SiO_2$ than on Ni/SiO_2. On the other hand, in the pressure range $p(CO) < 1.3$ kPa, the methanation rate on Ni/SiO_2 was proportional to $p(CO)$, but the rate on $Ni/Gd(1.5)/SiO_2$ still depended on $p(CO)^{-0.67}$. When CO adsorbs on Ni/SiO_2 without any coadsorbates, the adsorbed amount is saturated below 1.0 kPa. Thus the positive correlation between methanation rate and $p(CO)$ at $p(CO) < 1.3$ kPa over Ni/SiO_2 suggests that CO adsorp-

tion is blocked by hydrogen when $p(H_2) \gg p(CO)$. In contrast, no blocking of H_2 for CO adsorption was observed with $Ni/Gd(1.5)/SiO_2$, irrespectively of the smaller negative order with respect to CO pressure, as shown in Fig. 4. Adsorption sites of CO and hydrogen $Ni/Gd/SiO_2$ may be different from each other.

When $Ni/Gd/SiO_2$ was exposed to H_2, a new peak at 1610 cm^{-1} appeared. This peak disappeared by exposing to D_2 by the isotope exchange. We were not able to observe the isotope (D) band corresponding to the 1610 cm^{-1} peak as a low signal to noise ratio below 1300 cm^{-1}. The rate for the desorption of hydrogen was measured by mass spectrometry and from the decrease in intensity of the 1610 cm^{-1} peak by IR, giving the similar values of 4.0×10^{-11} and 4.3×10^{-11} mol s^{-1}, respectively, at 433 K. Hence the band at 1610 cm^{-1} is attributed to adsorbed hydrogen.

IR bands of hydrogen adsorbed on Ni metal have been reported to appear at 1200–700 and 600 cm^{-1} for threefold and fourfold hydrogen, respectively (*28*), and it does not appear around 1610 cm^{-1} (*29*). The intensity of the 1610 cm^{-1} band gradually increased when the sample was exposed to hydrogen at 407 K and its increase was very slow at 300 K. Hydrogen is known to be dissociated immediately on Ni metal surface with almost no activation barrier. From the behaviors of hydrogen on Ni metal and $Ni/Gd/SiO_2$, the band at 1610 cm^{-1} is assignable to a Gd–H stretching peak, where hydrogen atoms on the Ni metal surface migrate to partially reduced GdO_x in the $Ni/Gd/SiO_2$ catalyst. This also agrees with the fact that IR bands of Zn–H and Zr–H stretching vibrations have been observed at 1709 cm^{-1} (*30*) and 1562 cm^{-1} (*31*), respectively.

When the $Ni/Gd(1.5)/SiO_2$ catalyst was exposed to CO without evacuating hydrogen at 403 K (Fig. 9), the intensity of the 1610 cm^{-1} peak increased rapidly. The frequency of this band did not depend on the carbon isotopes of CO, excluding the possibility of the contribution of the side-on CO peak to the peak enhancement. In fact, the desorption measurements of hydrogen by mass spectrometry showed an increase in the amount of hydrogen adsorbed in the coexistence of CO. Thus the enhancement of the peak intensity at 1610 cm^{-1} corresponds to an increase of hydrogen atoms on GdO_x. This increase of Gd–H may be caused by the replacement of hydrogen adsorbed on Ni bare metal surface by adsorbed CO, resulting in the movement of H atoms to GdO_x. Partially reduced GdO_x acts as a hydrogen reservoir and keeps a high density of surface hydrogen under reaction conditions.

In addition to the repulsive interaction between CO and hydrogen on Ni bare metal surface, a positive interaction was also observed. The amount of CO adsorbed increased by hydrogen coadsorption. This phenomenon was also observed on Ni/SiO_2 catalyst, but the degree of the increase was larger with $Ni/Gd/SiO_2$ than on Ni/SiO_2. H–CO interaction has been observed on Ni(100) (*32, 33*), where both H and CO adspecies are stabilized. As the amount of hydrogen adsorbed on $Ni/Gd/SiO_2$ is larger than that on Ni/SiO_2, $Ni/Gd/SiO_2$ would have more interaction of adsorbate.

4. Promoting Effect of Gd Additive

Ni particles are interacted with partially reduced GdO_x as already discussed. At the boundary sites of GdO_x on Ni particles the side-on CO (Ni–C═O–Gd) is produced, exhibiting the peak of 1600 cm^{-1}. The dissociation probability of the side-on CO is almost 100% under reaction conditions. On the contrary, the dissociation of on-top and bridge CO is negligible. Surface carbides originated from the side-on CO were a little more active for the methanation than other carbides originating from on-top and bridge CO, but the difference was not significantly large.

Another effect of gadolinium is to reserve hydrogen on GdO_x under reaction conditions. Hydrogen density on $Ni/Gd/SiO_2$ under reaction conditions was higher than that on Ni/SiO_2; an IR band of 1610 cm^{-1} was

observed for Gd–H and 0.14 μmol g_{cat}^{-1} of hydrogen was adsorbed on Ni/Gd(1.5)/SiO_2 in the steady state of the reaction. Additionally, the adsorbed hydrogen increased the amount of CO adsorbed.

As discussed above, two promoting effects of GdO_x are observed on the Ni/Gd/SiO_2 system; one is the promotion of CO dissociation and the other is hydrogen storage. Under reaction conditions at 558 K, 5.1 and 2.0 μmol g_{cat}^{-1} of carbides remained on Ni/Gd(1.5)/SiO_2 and Ni/SiO_2 surfaces, respectively. The amount of carbides on Ni/Gd(1.5)/SiO_2 is 2.5 times as large as that on Ni/SiO_2. The overall reaction rate of CO hydrogenation on Ni/Gd/SiO_2 at 558 K (244 μmol min^{-1} g_{cat}^{-1}) was ca. five times as fast as that on Ni/SiO_2 (50.5 μmol min^{-1} g_{cat}^{-1}). If the rates are normalized to the amount of carbides, the rate of hydrogenation of carbides on Ni/Gd(1.5)/SiO_2 is two times larger than that for Ni/SiO_2. This promotion of Gd additive is ascribed to the hydrogen storage effect of GdO_x. On the basis of the amounts of CO adsorbed on Ni/Gd(1.5)/SiO_2 and Ni/SiO_2 under reaction conditions at 558 K, the rate constant for CO dissociation on Ni/Gd(1.5)/SiO_2 was ca. five times larger than that on Ni/SiO_2. Thus, the promoter effect of Gd is observed more with CO dissociation.

While the rate decrease in the low-CO-pressure range was observed with Ni/SiO_2, if molecularly adsorbed CO plays a key role in methanation, the linear phenomenon observed with Ni/Gd/SiO_2 in Fig. 4 cannot be a weaker dependency of the reaction rate on CO pressure compared with the case of Ni/SiO_2. The role of a Gd additive in the easy dissociation of CO through the side-on CO is also seen in Fig. 3. CO adsorption becomes more difficult at higher temperatures, leading to a rate decrease, whereas more rapid dissociation of CO on Ni/Gd/SiO_2 gives rise to linear dependency without a break over whole reaction temperatures.

CONCLUSIONS

(1) Gd exists as partially reduced GdO_x in Ni/Gd/SiO_2.

(2) GdO_x displays two promoter effects on the Ni catalysis for CO hydrogenation. One is the promotion of CO dissociation and the other is the enhancement of hydrogenation rate of carbides because of the storage of hydrogen (ν(Gd–H) = 1610 cm^{-1}).

(3) These two effects, consequently, increased the methanation rate, particularly at high temperatures.

(4) Side-on CO (Ni–C=O–Gd) is produced at the boundary sites of GdO_x on Ni particles, showing ν(CO) of 1600 cm^{-1}.

(5) All side-on CO species easily dissociate, whereas on-top and bridge CO species scarcely dissociate and most of them are desorbed by heating in vacuum.

(6) The amount of side-on CO was one-fifth as large as those of on-top and bridge CO on Ni/Gd(1.5)/SiO_2.

(7) Carbides originated from side-on CO were active for hydrogenation to produce hydrocarbons (mainly methane).

(8) It is suggested that adsorbed CO and hydrogen interact with each other to increase their adsorbed amounts.

REFERENCES

1. Sudhakar, C., and Vannice, M. A., *J. Catal.* **95,** 227 (1985).
2. Vannice, M. A., Sudhakar, C., and Freeman, M., *J. Catal.* **108,** 97 (1985).
3. Rieck, J. S., and Bell, A. T., *J. Catal.* **99,** 278 (1986).
4. Deboy, J. M., and Hicks, R. F., *J. Catal.* **113,** 517 (1988).
5. Oh, S. H., *J. Catal.* **124,** 447 (1990).
6. Kienneman, A., Breault, R., Hinderman, J.-P., and Lanrin, M., *J. Chem. Soc. Faraday Trans. 1* **83,** 2119 (1987).
7. Underwood, R. P., and Bell, A. T., *J. Catal.* **111,** 325 (1988).
8. Takahashi, N., Mori, T., Miyamoto, A., Hattori, T., and Murakami, Y., *Appl. Catal.* **38,** 61 (1988).
9. Dictor, R., and Roberts, S., *J. Phys. Chem.* **93,** 5846 (1989).
10. Jin, T., Zhou, Y., Mains, G. J., and White, J. M., *J. Phys. Chem.* **91,** 5931 (1987).
11. Wentrcek, P. R., Wood, B. J., and Wise, H., *J. Catal.* **43,** 363 (1976).
12. Araki, M., and Ponec, V., *J. Catal.* **44,** 439 (1976).
13. Zhao, Y., and Chung, Y., *J. Catal.* **106,** 369 (1987).
14. Zhao, Y., and Chung, Y., *J. Catal.* **124,** 109 (1990).
15. Chen, J. G., Crowell, J. E., Ng, L., Basu, P., and Yates, J. T., *J. Phys. Chem.* **92,** 2574 (1988).

16. Chen, J. G., Crowell, J. E., and Yates, J. T., *Surf. Sci.* **187,** 243 (1987).
17. Shido, T., Asakura, K., and Iwasawa, Y., *J. Catal.* **122,** 55 (1990).
18. Shido, T., and Iwasawa, Y., *J. Catal.* **129,** 343 (1991).
19. Nishimura, M., Asakura, K., and Iwasawa, Y., Proceedings, 9th International Congress on Catalysis, Calgary, 1988'' (M. J. Philips and M. Ternan, Eds.), Vol. IV, p. 1842. Chem. Institute of Canada, Ottawa, 1988.
20. Sasaki, T., Aruga, T., Kuroda, H., and Iwasawa, Y., *Surf. Sci.* **240,** 223 (1990).
21. Shido, T., Asakura, K., and Iwasawa, Y., *J. Chem. Soc. Faraday Trans. 1* **85,** 441 (1989).
22. Yates, J. T., and Garland, C. M., *J. Chem. Phys.* **65,** 617 (1961).
23. Primet, M., Dalmon, J. A., and Martin, G. A., *J. Catal.* **46,** 25 (1977).
24. Martin, G. A., Primet, M., and Dalmon, J. A., *J. Catal.* **53,** 321 (1987).
25. Erley, W., Ibach, H., Lehwald, S., and Wagner, H., *Surf. Sci.* **83,** 585 (1979).
26. Canpuzano, J. C., and Grennler, R. G., *Surf Sci.* **83,** 301 (1979).
27. Anderson, S., *Solid State Commun.* **21,** 75 (1973).
28. Christmann, K., *Surf. Sci. Rep.* **9,** 1 (1988).
29. van Hardeveld, R., and Hartog, F., *Adv. Catal.* **22,** 75 (1972).
30. Eischens, R. P., Pliskin, W. A., and Low, M. J. D., *J. Catal.* **1,** 180 (1962).
31. Kondo, J., Sakata, Y., Domen, K., Maruya, K., and Onishi, T., *J. Chem. Soc. Faraday Trans.* **86,** 397 (1990).
32. Westerlund, L., Jönsson, L., and Anderson, S., *Surf. Sci.* **199,** 109 (1988).
33. Li, J., Schiøtt, B., Hoffmann, R., and Proserpio, D. M., J. Phys. Chem. **94,** 1554 (1990).